https://doi.org/10.1016/j.jclepro.2021.126116

6513 words

Strategic Planting for Watershed Restoration in Coastal Urban Environment – Toward Carbon Sequestration by Stormwater Improvement

Xiaojing Tang[a], Ka-Lai Chan[a], Shazia Farzana[a], Onyx W.H. Wai[a,b], and Shao-Yuan Leu[a,b,c*]

[a] Department of Civil and Environmental Engineering, The Hong Kong Polytechnic University, Hung Hom, Kowloon, Hong Kong SAR;

[b] Research Institute for Sustainable Urban Development (RISUD), The Hong Kong Polytechnic University;

[c] Research Institute for Smart Energy (RISE), The Hong Kong Polytechnic University;

[*] Correspondence: Department of Civil and Environmental Engineering, the Hong Kong Polytechnic University, Hung Hom, Kowloon, Hong Kong SAR; Phone: 852-3400-8322; Fax: 852-2334-6389; E-mail: syleu@polyu.edu.hk (S,-Y. Leu)

Highlight

- Carbon sequestration potentials of 21 plant species were studied upon the water purification benefits in watershed restoration;
- Half-life coefficients of NH_4^+ degradation showed negative relationship with increasing leaves and shoot biomass;
- Optimal riparian planting can reduce GHGs emission from 0.151 to 0.082 kg CO^2-e/m^3 water treated;
- Improper riparian planting increased GHGs emission by 16.5%.

Abstract

Organic compounds and nutrients in urban runoff create negative impacts to global warming. Riparian planting (RP) of urban watershed carried out only for urban greening may induce the degradation of pollutants, while fixing the carbon and nitrogen in plant biomass. While a few previous publications have demonstrated the potential benefits of stormwater treatment by RP, the critical plant-specific indexes and corresponding contributions to the reduction of greenhouse gas (GHG) emission, in both the senses of water purification and carbon fixation, have never been elucidated quantitatively. This study investigated a total of 21 plant species to their capacities reducing carbonaceous pollutants and NH_4^+ in synthetic stormwater during a 30-day period and under different operational conditions. Water quality data were collected to analyze the half-life ($t_{1/2}$) of pollutants degradation rates of each species. Carbon contents in the stem, leaf and root of each species were also measured and used to calculate the total carbon sequestration potential per planting area. *Colocasia tonoimo (CT)* and *Thalia dealbata* in freshwater; *Crinum asiaticum* and *Phragmites australis* in brackish water; and *Kandelia obovate*and *Aegiceras corniculatum* in seawater showed shortest average $t_{1/2}$ for the degradation of all three pollutants. Closed negative correlation were found between the $t_{1/2}$ of NH_4^+ and the increased biomass in leaves and shoot. The highest carbon sequestration density was the highest using plant *CT*, in both batch and continuous flow systems, *i.e.*, 231.1 and 313.9 g/m^2, respectively. Nitrogen sequestration density of *CT* in batch and continuous conditions were 16.7 and 22.6 g/m^2, respectively, which was also the highest among all the tested species. Current GHG emission of the targeted watershed without planting (Tsui Ping River, Hong Kong) were 0.151 kg CO_2-e/m^3-water. When CT were planted in the simulated watershed at the maximum areas, the GHG emission can be reduced to 0.082 kg CO_2-e/m^3.

Keywords: water-energy nexus; stormwater treatment; riparian planting; watershed management; greenhouse gas emission

List of Nomenclature

A	*Clerodendrum inerme*
AC_a	*Acorus calamus*
AC_c	*Aegiceras corniculatum*
AI	*Acanthus ilicifolius*
AM	*Alocasia macrorrhizos*
APA	*Alisma plantago-aquatica*
BG	*Bruguiera gymnorrhiza*
BMPs	Best management practices
Cp	Total carbon stock
CD	*Commelina diffusa*
COD	Chemical oxygen demand (mg/L)
CrA	*Crinum asiaticum*
CT	*Colocasia tonoimo*
CW	Constructed wetland
CyA	*Cyperus alternifolius*
DO	Dissolved oxygen (mg/L)
EF	Emission factors
EH	*Equisetum hyemale*
F	*Acrostichum aureum*
FIP	Floating island planting
GHG	Greenhouse gas
GWP	Global warming potential (kg CO_2-e)
JE	*Typha orientalis*
KO	*Kandelia obovata*
PA	*Phragmites australis*
PM	*Panicum maximum*
RP	Riparian planting
SC	*Saururus chinensis*
SS	*Scaevola sericea*
$t_{1/2}$	Half-life coefficient for pollutant degradation (day)
TD	*Thalia dealbata*
TOC	Total organic carbon (mg/L)

1. Introduction

The development of a circular economy relies on comprehensive integration of energy, water and environmental systems (Baleta et al., 2019). Under this prospective, watershed restoration has played a significant role for both regional and global environmental measures during urbanization (Lin et al., 2020). Through the removal of concrete structure and enhanced plantation, urban watersheds provide many direct and indirect values in the social (Chen and Cho, 2019), ecological (Zheng et al., 2019), and environmental perspectives (Sharrock and Jackson, 2017); in addition to their conventional functions of flood and sediments attenuation (Hu et al., 2019). The modern watershed restoration strategies, such as instream structure placement, riparian planting (RP), road restoration, and reconnection of isolated habitats have been extensively applied to reestablish interactions among ecosystem components and environmental disturbances (Ralston and Sarr, 2017). Applications of green structures with aquatic systems, such as the constructed wetlands (CW) (Baleta et al., 2019), rain garden (Pavolová et al., 2019), best management practices (BMPs) (Xu et al., 2019) or other green infrastructures (Nordman et al., 2018) have also been widely considered in watershed management.

Stormwater runoff is a main contributor of non-point source pollution (Chandrasena et al., 2017). Organic matters, suspended particles, heavy metal or even micro-plastics in stormwater can directly threaten aquatic lives or gradually affect the whole ecosystem in the long run (Davis et al., 2009). Urban stormwater may also contain high nitrogen nutrients originated from fertilizer or putrescible wastes (Lopez-Ponnada et al., 2020). To control the water quality of stormwater runoff and reduce the total pollutant loads into the receiving water bodies, floating island planting (FIP) and RP have been applied as emerging best management practices (BMPs) for watershed restoration. Those systems can remove pollutants through hydraulic retention and biological activities (Loperfido et al., 2014), and vegetation has been employed in pollutants degradation (Breen, 1990). Appropriate planting can promote water purification with minimal management (Rogers et al., 1991). For example, Revitt et al. (1997) developed a reedbed treatment system to treat airport runoff and reported a chemical oxygen demand (COD) reduction of 31% (with a mean influent concentration of 47 mg/L) and NH_4^+ reduction of 28%, respectively. Yang et al. (2008) examined the performance of a floating emergent macrophyte treatment wetlands mesocosm receiving artificial agricultural runoff (influent COD 42-69 g/m^3) at different loading rates, and reported a consistent background COD concentration in the effluent of 35-40 g/m^3 regardless of the residence time (1-3 days) or influent loading rate (7.5-37.3 g/m^2 /day). Ladislas et al. (2013) investigated plant species in floating treatment wetland for metal and organic matter removals from stormwater, resulting in a significant COD drop from 132 mg/L to 72.6 mg/L. Li et al. (2017) reported that stormwater treatment using an aquatic retention pond followed by a horizontal subsurface flow construction wetland (CW) achieved reasonable removal efficiencies of 79.2% and 56.5% for COD and NH_4^+, respectively. The system was carried out with plantation operated at hydraulic retention time of 1.8-3.5 days and the influent flow contained low concentrations of pollutants, i.e., approximately 38.6 mg/L COD and 0.8 mg/L NH_4^+.

The impacts of water purification to sustainable development have been quantified by carbon footprint or global warming potential (GWP) analyses (Zhuang et al., 2020a). Methane and nitrous oxide are major greenhouse gases (GHGs) that can be generated from polluted water. Biodegradation of COD depleted dissolved oxygen (DO) and the resulted uncontrolled anaerobic digestion of the organics increased methane production (Rosso and Stenstrom, 2008). Unexpected discharges of nutrients may result in the production of nitrous oxide, and eutrophication may further aggravate the production of those undesirable gases (Perrin et al., 2017). Improvement in carbon and oxygen balance is expected with the introduction of urban vegetation to the watershed. Plants can consume or absorb the pollutants and nutrients, store carbon in the biomass, and mitigate the oxygen balance through photosynthesis. However, the carbon sequestration potential of different plant species may vary significantly among various planting or operational conditions. Most of the previous studies have considered only the greening facility (*e.g.*, rain garden) as a whole treatment unit, and no comprehensive quantitative measures on plant selection have been conducted. The plant-specific relationships between biomass accumulation over water purification under the influences of different tidal situations and changed salinity have never been clarified.

The goal of this study was to study the carbon sequestration potential of various plant species in a river/marine environment. An urban watershed Tsui Ping River in Hong Kong was applied as a study background before its restoration. A total of 21 plant species of concerns in the watershed, including mangroves, shrubs, and herbs were grown in lab-tanks and fed with controlled carbonaceous pollutants and nutrients. We applied a pot trial under controlled conditions to address the following questions, *i.e.*, (a) Does the presence of vegetation reduce pollutant concentration in the stormwater effluent? (b) Does flow pattern influence pollutants removal? (c) Is there any correlation between pollutants removal and plants growth? (d) How much carbon sequestration does plantation contribute? The growing conditions were designed to simulate the field conditions, including tidal differences, salinities, and water flow. The concentrations of the pollutants in the testing water were monitored closely over time to understand the dynamic changes of pollutants degradation; and the biomass were weighted by sections after the experiments. The information was applied in the calculation of GWPs using the targeted watershed as background. The possible impacts of the carbon balance were rated upon four designed scenarios with various levels of plantation and species to clarify the sensitivity of the related practice to GHGs emissions.

2. Material and Method

2.1 Background of the studied watershed

Tsui Ping River is a typical water channel receiving high organic pollutants from the domestic outfalls (**Figure 1**, top). The average flow rate is approximately 57508 m^3/d; and the COD, NH_4^+ and DO were 28.35, 1.04 and 7.16 mg/L, respectively. A comprehensive restoration project was proposed to upgrade the aquatic environment; for which the nullah has been divided into 3 zones from upstream to downstream for restoration, including a freshwater zone (Zone A), a brackish water zone (Zone B) and a seawater zone (Zone C). Salinity in the river gradually increased from Zone C to Zone A as upstream connects with inland freshwater resource and downstream flows to ocean. Three designs for embankment construction were proposed with increasing areas for plantation: Design I illustrates current profile; Design II constructs a platform for cultivation and Design III leaves all area of slop for planting where intersection angle between slop and horizontal is approximately 45°and floating island also exist in the middle of river. The area alongside river is currently 2,742.78 m^2. In addition, floating islands with total planting area of 696.5 m^2 will be constructed in the middle of the river for Design III.

2.2 Experimental set-up

Lab-scale water tanks were constructed with dimensions of 150 cm length, 30 or 40 cm width, and 50 cm height for water purification experiments (**Figure 2**). The differences of 40 cm and 30 cm in width were applied for comparatively the bigger tree/shrub species and smaller herbal species, respectively. A total of nine same plant species were evenly placed in a tank. The water depth from the soil surface was approximately 10 cm, and the basic plant set-ups of three studied zones are shown in **Table1**. Synthetic stormwater with 16.4 mg/L ammonia, 164 mg/L peptone and 44 mg/L glucose, was employed in the experiments. In order to match the changed salinities in different zones, 0 ppt, 5 ppt and 15 ppt concentrations of coral salts were employed in the synthetic stormwater in Zones A, B and C, respectively. To provide consistent lighting, natural and artificial light were carefully balanced and adjusted to provide homogenous luminous flux in different testing tanks. The temperature of the room has been fixed at 25°C throughout the testing period. To simulate the tidal effects to plant growth and water purification capacities, the tested plants were kept in water at low tide for 18-16 hours and taken out from the water for 6-8 hours at high tide. The batch experiments (with static flow) and continuous flow experiments (with flow rate of 3-8 L/s) were conducted simultaneously, where pump originated power to support continuous flow experiments.

A total of 21 plant species potentially suitable planted in different salinity of stormwater were chosen and investigated, of which *Colocasia tonoimo* (Chan et al.), *Panicum maximum* (PM), *Saururus chinensis* (SC), *Acorus calamus* (AC_a), *Thalia dealbata* (TD), *Alocasia macrorrhizos* (AM), *Alisma plantago-aquatica* (APA) were chosen for Zone A; *Typha orientalis* (Viana et al.), *Juncus effuses* (Kauffman et al.), *Crinum asiaticum* (CrA), *Commelina diffusa* (CD), *Cyperus alternifolius* (CyA), *Phragmites australis* (PA) were tested in Zone B; and high saline species, *Aegiceras corniculatum* (AC_c), *Kandelia obovate* (Baleta et al.), *Bruguiera gymnorrhiza* (BG), *Acanthus ilicifolius* (AI), *Acrostichum aureum* (F) and *Clerodendrum inerme* (A) were used in Zone C, where most of the plants were true mangroves. Before experiments, the plant species employed in Zone A, B and C were cultivated in 0 ppt, 5 ppt and 15 ppt saline water with pollutant-free condition for 15 days. After 15-days of acclimation, experiments started and synthetic stormwater was added into each tank. As soon as experiments launched, water sample in each tank would be taken at day 0, day 1, day 3, day7, day 15, and day 30 for analysis.

2.3 Physical properties

Plant height and leaf number of each plant species were recorded with water quality tests. The biomass of the individual plant was measured by the following process. The fresh biomass of each part (leaf, stem and root) of the plant was measured separately immediately after segregation. After taking fresh biomass measurements, every part of the plant was taken for dry weight measurements. The samples were oven-dried at 80 °C until constant weights. The total dry biomass weight of each plant was calculated by summation of the weight of all the samples.

2.4 Chemical analysis for stormwater

Water samples were collected and passed through 0.45 μm pore size filter. The filtrates were employed for total organic carbon, chemical oxygen demand (COD) and NH_4^+ measurement. The concentrations of TOC were measured by TOC analyzer. COD were tested by COD kit. In brief, 2 ml synthetic stormwater samples were added in the COD kit, and the mixtures of the solution were in pre-heated digester at 150 ℃ for 2 hours. The color absorbance was measured at 410 nm using UV-VIS spectrophotometer. The concentrations of NH_4^+ of the synthetic storm water samples were measured using direct nesslerization method. In brief, 0.8 mL potassium sodium tartrate was added into 0.6 mL synthetic storm water samples to prevent calcium and magnesium from precipitating with nessler reagent, followed by the addition of 0.8 mL nessler reagents and diluted to 5 mL. The mixture was kept for 10 minutes to develop yellow colors, the absorbance of the mixtures was measured at 420 nm using UV-VIS spectrophotometer. This method is slightly different from the methods used in Zone C, of which 1 mL nessler reagents were added in 0.2 mL synthetic storm-water samples and dilute to 5 mL. Since precipitation can increase ammonia absorbance at 420 nm, extra potassium sodium tartrate was added to prevent calcium and magnesium from reacting with nessler reagent, resulting in relatively more accurate ammonia value. DO was measured by DO meter.

2.5 Data analysis

2.5.1. Pollutants degradation half-life

Plant species can remove pollutants with high efficiency, which attributing to combined effect of entire plant biomass, instead of effect of unit plant biomass. For example, pollutants may be degraded faster by bigger plants than the smaller ones, although pollutants degradation capacity of unit biomass of bigger plant species were less than that of smaller plant species. Thus, the pollutants per unit dry biomass were calculated to compare species. A 2^{nd} order kinetic model was used to simulate TOC and COD per unit dry biomass. Exponential model was used to fit NH_4^+ per unit dry biomass by various species. To compare the removal capacities of the pollutants among all the plant species, the half-life would be developed according to equation of models. The relationship between half-life of pollutant (COD, TOC and NH_4^+) degradations per unit biomass and segregated parts of unit biomass were investigated to standardize the comparisons.

2.5.2. Carbon sequestration densities in plants

The 21 plant species employed in this study consisted of herb, shrub and tree, which contained various carbon contents due to tissue differences. Chan et al. (2018) provided a comprehensive method on carbon sequestration potentials with different plant species after chemical composition analyses, of which the related parameters were applied in this study. The total carbon stock (C_p) in individual plant can be calculated by Equations (1):

$$C_p = (M_l \cdot f_l + M_s \cdot f_s + M_r \cdot f_r) \cdot \rho \quad (1)$$

where M_l, M_s and M_r are the increased dry biomass of leaves, stem and root in a plant, respectively (g); ρ is the population density of plant biomass per unit area (stand·m^{-2}); f_l, f_s and f_r represent the carbon content of leaves, stem and root, respectively, where except f_l and fs for shrub and tree were calculated based on Chan et al. (2018) (f_l of shrub = 0.19, f_l of tree = 0.21, f_s of shrub = 0.31, an f_s of tree = 0.32), f_r, f_l and f_s for herb, shrub and tree was extracted from Ma et al. (2018), where f_r, f_l and f_s for herb equal to 0.4245, 0.4473 and 0.4241, respectively, f_r for shrub and tree is 0.4743.

2.5.3. Nitrogen sequestration density in plants

Reich et al. (2006) provided a method to calculate the nitrogen content in herb and tree. Nitrogen content in shrub could be obtained from Viana et al. (2012). Increased N mass in shrub ($M_{N-shrub}$) can be calculated by equation (2):

$$M_{N-shrub} = 0.8725\%\, M_{shoot} + 0.6675\% M_{root} \quad (2)$$

Where $M_{N-shrub}$ is increased N mass of shrub (g); M_{shoot} (g) and M_{root} (g) are dry increased shoot and root biomass of shrub over 30 experimental periods, respectively. The accumulated N mass in tree and herb can be obtained by Equations (3) and (4), respectively:

$$M_{N-herb} = M^{1.003}/10^{1.517} \quad (3)$$

$$M_{N-tree} = M^{0.945}/10^{2.197} \quad (4)$$

where M_{N-herb} and M_{N-tree} are increased N mass of herb and tree (g), respectively; M is dry increased biomass (g). Based on above equations, the nitrogen sequestration density of each plant pecies was obtained.

2.5.4. Emission factors and greenhouse gas inventories

Three watershed restoration scenarios to reconstruct the embankment by Hong Kong SAR government were demonstrated (**Figure 1,** bottom), of which Design (I) is the current profile of embankment; Design (II) constructs a platform for cultivation and Design (III) leaves all area of slop for planting. Given that the area of embankment in vertical view in Tsui Ping River is 2742.78 m^2, the area of platform in design B equals to 2743 m^2, while the area of slope in Design (III) is 4575 m^2 since intersection angle between slop and horizontal is approximately 45° and floating island of 696.51 m^2 also exist in the middle of river. Surface of embankment of design A is laid concrete, so that no vegetation grows on it. Engineers designed a layer of hexagonal-ring shaped bricks in design B, and central space of brick left for planting without covered by bricks. In Design (III), the whole slop area is filled with soil for planting vegetation. According to Hong Kong standard, naked planting area is approximately 1.2 times of available planting part of hexagonal-ring shaped bricks. In other words, planting density of Design (III) is 1.2 times of Design (II).

The results of carbon sequestration density showed that CT and EH were the highest and lowest (**Table 2**). We would select CT and EH to estimate the minimum and maximum GHGs emission with 3 embankment designs. Four scenarios which would be discussed about potential GHGs emission were shown in **Table 3**. Vegetation growth can help carbon and nitrogen fixation from external environment, decreasing potential GHGs emission. Inherent DO contained in Tsui Ping River have potential to offset a part of COD.

The GHGs emission factors (EF) of different emission sources are listed in **Table 4**. The reduced GHGs from carbon and nitrogen sequestration were taken as 3.67 kg CO_2/kg C stock and 3.14 kg N_2O /kg N stock, respectively, through dividing CO_2 molecular mass by C mass and dividing N_2O mass by N mass. The value of reduced CH_4 by DO was 0.25, equaled to value of CH_4 from COD, since unit mass DO can offset unit mass COD. The GHGs emissions from receiving water were calculated based on the potential impacts of unexpected methane emissions due to anaerobic reaction and eutrophication. The EF of GHGs is used to calculate the GHGs emissions per unit of available activity. The total GHGs emissions were calculated by Equation (5) as:

$$E = \sum_{i=1}^{n} A_i \times EF_i \times GWP_i \quad (5)$$

where E = total emissions in CO_2 equivalent (kg CO_2-e·m^{-3}); i = selected sources of a GHG; A_i = activity of GHG i; EF_i = Emission Factor of GHG i; and GWP_i = Global Warming Potential of GHG i for a 100-year time horizon obtained from IPCC's Fifth Assessment Report; and n = total type of GHGs in discuss.

3. Results and discussion

3.1 Physical properties among different plant species

The physical plants properties in batch and continuous experiments are presented in (**Figure 3**). For plant species in Zone A, the heights of plants showed a wide variation from 39.3 cm to 127.4 cm at the day 30 and the height in batch and continuous experiments were similar. All the plant heights at day 30 were lower than that at day 0. Leaf number of all plant species were nearly same except for SC. Leaf number of SC by day 30 in batch experiment were 47.4 and accounted for roughly half of that in continuous experiment of 73.9. In general, almost dry biomass weight of plants in continuous was more than that in batch. This phenomenon indicated that plant species in continuous were preferable for plant cultivation.

In Zone B, the heights of plant were ranged from 13.75 cm (CrA) to 71.42 cm (JE) at day 30. Among the heights of all plant species throughout the whole experimental period, height of CrA gained the maximum increase of 186% and 47% in batch (from 9.3 cm to 26.72 cm) and continuous experiments (from 9.3 cm to 13.8 cm), respectively. EH showed the highest reduction rate of 38% in height in both batch and continuous flow experiments, respectively, which was decreasing from initial 56.4 cm and 55.7 cm to 34.8 cm and 34.7 cm by day 30. Leaf number at day 30 showed a wide variation from 6.3 to 116.3. The maximum falling of leaves was observed in CD, whose average leaf number in batch and continuous experiments reduced from 191.4 and 227.5 to 96.3 and 116.3, respectively. CD showed height reduction rate up to 32% compared to initial value. CD was observed to be intolerant to the 5 ppt saline water early in the acclimation period (*i.e.*, no pollutants). To confirm the observation, two pots of CD were tested in freshwater with the same simulated tidal cycle, and both pots stayed healthy for a much longer time. Thus, the salt intolerance can explain why CD showed high reduction in height and leaf number. There was a litter difference between numerical value in batch and continuous experiments. Initial biomass of CyA, TO and EH decreased from 51.37 g, 32.59 g and 67.75 g to approximately 32 g, 20 g, and 33 g in both batch and continuous experiments by the end. But biomass of PA, SS and CrA showed a significantly increase rate of 290%, 113% and 265%, respectively. Those plant species grew from approximately 5.2 g, 8.9 g, and 9.12 g to 20.0 g, 18.9 g, and 33.0 g, respectively.

For plant species in Zone C, the highest value was obtained from A whose height was more than 70 cm throughout whole experimental period. All height of plant species kept relatively stable throughout 30-day growing, except height of F which dropped from 53.8 cm to 42.9 cm in batch experiment and decreased from 34 cm to 29.95 cm in continuous experiment. In both batch and continuous experiments at day 30, the leaf number varied from 8.6 to 66. Compared to initial value, average leaf number reduced 9.5% and 1.9% in batch and continuous experiments. Dry biomass of almost plant species ranged from 4.1 g to 59.0 g.

The data of the plant growth provided important information to the growth of different plant species in a well-controlled environment. While beyond the scope of this study, the variation in plant growth, under the laboratory and field environment, is of critical and well-addressed in some previous studies. Rozema et al. (1997) compared chambers studies and field experiments with various UV-B radiations on plant metabolisms, and indicated that plant growth could be less sensitive in field conditions than in laboratory. Reich et al. (2006) studied laboratory and field results of 43 field grown plants species and investigated the impacts of changing growing conditions on plant respiration. The relations between whole-plant respiration and biomass for plants in contrasting environments (high versus low light, differing atmospheric CO_2 concentration, temperature, and nitrogen supply) or different functional groups had similar scaling slopes, while total nitrogen content showed stronger impact than other factors. For older, field-grown plants, whole-plant respiration rates at any given size were lower for the field-grown plants than the laboratory plants. In addition, both the field grown saplings and larger trees had much greater above-ground biomass at a common above-ground respiration rate than did the laboratory-grown plants.

3.2 Pollutant degradation half-life ($t_{1/2}$)

The result of three pollutants (COD, TOC and NH_4^+) in stormwater had been measured and recorded in day 0, 1, 3, 7, 15, 30, 45, and 60. Pollutants per dry biomass in batch experiment had also been calculated signed by dot (**Figure 4**). Due to difference of dry biomass of plant species, initial value of pollutants removal per unit biomass were located at various site of Y-axis, although initial pollutants concentrations (TOC, COD and NH_4^+) among tanks were same. Pollutants per unit biomass fitting curves were constructed based on calculated data, represented by dash lines. The parameters of equation of all fitting curves were showed in **Table 5**, where almost R^2 of equation ranged from 0.85 to 0.98 and showed reliable fitting. The 2nd order model was more applicable to COD and TOC per unit dry biomass than other models, while fitting curve of NH_4^+ per unit dry biomass could have maximum R^2 when it was simulated by exponential equation. Particularly, TOC in continuous and COD in both flow patterns treated by AI; TOC and COD in both flow patterns treated by F performed poor fitting by all models. It was observed that leaves of F were shrinkage from day 7 to the end, and leave of AI fell and yellowed stared from day 7. These poor growth condition of F and AI may cause irregular pollutants per unit dry biomass and invalid fitting.

According to the curve fitting equations and their parameters, half-life coefficients ($t_{1/2}$) of each species were calculated for the degradation of three pollutants by 21 plant species in synthetic stormwater were revealed in **Figure 5**, of which **Figure 5** (a) and (d) described $t_{1/2}$ of TOC, COD and NH_4^+ treated by seven species in Zone A, including CT, PM, SC, AC^a, TD, AM and APA. In both of batch and continuous experiments, $t_{1/2}$ by all species followed the order of NH_4^+ > TOC > COD. The results indicated COD were the easiest to remove ($t_{1/2}$ of COD ranged from 0.81 to 2.26 days), and NH_4^+ require longer time to degrade than other two pollutants ($t_{1/2}$ of NH_4^+ ranged from 6.38 to 12.20 days). Compared to $t_{1/2}$ of NH_4^+ and TOC in batch experiments, $t_{1/2}$ in the continuous experiments were obviously shorter. There was no large difference between $t_{1/2}$ of COD in batch and continuous experiments, since numerical half-life in both flow patterns were short enough, while TOC and NH_4^+ required longer time to decay with more distinct gap between batch and continuous flow. Meanwhile $t_{1/2}$ of COD in Zone B & C in continuous experiments were obviously shorter than that in batch experiment. The results suggested that continuous flow can promote pollutants degradation in synthetic storm water. DO (**Table 5**) in continuous flow was higher than that in steady water (batch experiments), which provide more oxygen to oxidize organic compounds to inorganic compounds and support nitrification process (NH_4^+ to NO_2^-). In this way, concentration of TOC and NH_4^+ in continuous experiment can be reduced quickly. In Zone A, $t_{1/2}$ of TOC in both flow patterns varied from 2.04 to 6.72 days, that of TD and CT were shorter than other species (3.46 and 2.04 days for batch and continuous of CT, respectively; 2.91 and 2.25 days for batch and continuous of TD, respectively). TD also can remove NH_4^+ with the fastest rate among all species in Zone A, whose $t_{1/2}$ was 6.47 and 6.50 days in batch and continuous experiments, respectively. All the average DO was higher in continuous experiments (**Table S2**) than the batch systems. Compared with conventional constructed wetland systems, the tidal flow system demonstrated greater efficiency in the removal of organic matter (Sun et al., 2005). Average oxygen supply under tidal operation (350 $g{\cdot}m^{-2}{\cdot}d^{-1}$) was much higher than in conventional constructed wetlands (<100 $g\ m^{-2}\ d^{-1}$), resulting in enhanced removal of BOD_5 and NH_4^+ (Wu et al., 2011). Similar appearance was observed in this study, half-life of pollutants (COD, NH_4^+ and TOC) were shorter in continuous than that in batch experiments.

The $t_{1/2}$ of pollutants treated in Zone B were shown in **Figure 5** (b) and (f). Eight species were cultivated with 5ppt salinity, consisting of TO, JE, CrA, SS, CD, CyA, EH and PA. $t_{1/2}$ of TOC varied from 1.65 to 5.70 days. CD, CyA and PA had higher removal efficiency of TOC, whose $t_{1/2}$

varied from 1.65 to 2.86 days. COD presented a considerable variation in $t_{1/2}$ (2.33 – 8.80 days). The shorter $t_{1/2}$ were from PA (2.75 days and 2.65 days for batch and continuous, respectively). NH_4^+ was the hardest pollutant to be removed compared to other two pollutants, whose $t_{1/2}$ ranged from 3.78 to 9.89 days, were longer than $t_{1/2}$ of other two pollutants. CrA ($t_{1/2}$ of 5.53 and 3.78 days for batch and continuous, respectively) and PA ($t_{1/2}$ of 4.83 and 3.9 days for batch and continuous) can remove NH_4^+ with the fastest rate than other species in Zone B. Among 8 species, TO and EH had lower pollutants (TOC, COD and NH_4^+) removal efficiency with longer $t_{1/2}$. We also observed that TO was infested by aphids, and the condition worsened during the experiment. Also, the long and thin leaves of TO were relatively prone to breaking and tangling, especially when wetted, and did not recover easily. The EH was quite stable in each experiment at very beginning where the stems started to shrink and brown from the tips. Small bladder snails were found in the EH tanks. Thus, TO and EH should be taken care and avoid them from insect pest threatening.

Six plant species, *i.e.*, KO, AC_c, BG, AI, A and F, were grown in synthetic stormwater with 15 ppt salinity of Zone C. The results of $t_{1/2}$ demonstrated in **Figure 5** (c) and (g). The $t_{1/2}$ of TOC ranged from 0.50 and 3.95 days, and the $t_{1/2}$ of NH_4^+ varied from 5.57 to 10.56 days. The range of $t_{1/2}$ of COD was much extensive than the other pollutants (from 27.19 to 75.08 days). Especially, biomass loss of AI was extremely significant, resulting in a negative $t_{1/2}$ of COD (not shown in the figure). AI have poor capability in COD removal, even possibly deteriorate aquatic quality. The half-life of TOC by F in batch and COD by AI in both batch and continuous experiments were also not presented herein, due to poor growing conditions. F were noted that leaves shrinkage from day 7 to end. This health condition may lead to disorder TOC and COD degradation and hence not considered in our discussion.

3.3 Correlation between half-life and segregated biomass

Given the results of segregated dry biomass of each species, including leaf, stem and root in both the starting and end dates the changes of dry biomass were calculated. The correlations between increased dry biomass (*i.e.*, total biomass, shoot biomass, leaves biomass and root biomass) and $t_{1/2}$ of tested pollutants (*i.e.*, TOC, COD and NH_4^+) had been presented in **Figure 6**. The $t_{1/2}$ of NH_4^+ in both of batch and continuous flow experiment were closely negative related to increased shoot biomass (ISB), displayed in **Figure 6** (a) (R^2 of batch experiment = 0.68, and R^2 of continuous experiment = 0.73). Besides, the $t_{1/2}$ of NH_4^+ showed closed negative correlation with increased leaves biomass (Roni et al.), demonstrated in **Figure 6** (b) (R^2 of batch experiment = 0.54, and R^2 of continuous experiment = 0.81). The finding confirmed the role of leaves and stem growth effect on mitigating NH_4+ pressure on aquatic environment. Previous study of Vymazal (1995) suggested that nitrogen can be taken up directly by shoots and be converted into organic compounds that serve as building blocks for cells and tissues. The rate of nitrogen removal is enslaved to the vegetation net productivity (growth rate), the concentration of nitrogen in the plant tissue (Ge et al., 2016; Keizer-Vlek et al., 2014). The results of this study confirmed that NH_4^+ may be transformed to serving stem and leaves growing. The intercept in continuous flow experiment is lower than that in batch experiment, suggesting that continuous flow can strengthen NH_4^+ decomposition that steady water. Continuous flow can blend and contain more oxygen from external environment, which can promote nitrification and decrease NH_4^+. The **Figure 6** (d) revealed that root biomass growth isn't significant related to $t_{1/2}$ of NH_4^+. However, Xu et al. (2017) pointed out that root biomass also can uptake nitrogen to build root productivity. This phenomenon was contrast with our results, since the plant species utilized in that paper were different with this study. There were no obvious correlations found between $t_{1/2}$ of TOC and COD with increased biomass, implying that NH_4^+ could be uptake by stem and leaves of plant species. When species reach maturation period, stem and leaves would stop growing and less NH_4^+ could be consumed by the vegetation. The results provided a strategy that harvest above-ground biomass can alleviate NH_4^+ pressure on aquatic environment. In terms of management strategies, nutrients in plant tissues can be removed through plant harvesting.

3.4 C and N sequestration density

The carbon and nitrogen sequestration densities of each species were shown in **Table 2**. C sequestration density is in the range from -432.86 to 313.9 g/ m^2. N sequestration varied from -31.35 to 22.64 g/m^2. Because some species got biomass loss, negative value of C and N sequestration density occurred. Among all species, carbon sequestration density in 30 days of CT was maximum, with 231.12 and 313.90 g/ m^2 in batch and continuous flow experiment, respectively, suggesting that CT has great potential of carbon fixation. N sequestration of CT was the highest, with 16.69 and 22.64 g/ m^2. The $t_{1/2}$ of three pollutants treated by CT was also shorter than most species. However, some species showed negative carbon sequestration density, implying that those species could strengthen carbon emission and worsen environmental issues induced by GHGs. EH was cultivated in Zone B with -95.68 and -128.2 g/m^2 carbon sequestration density in batch and continuous flow, respectively. It was observed that EH's stems shrink and browned from the tips and bladder snails were found in the EH. The insects may damage the EH's healthy condition, further caused biomass loss occurred. The results of carbon sequestration density provided planting strategies. Selecting species with higher carbon sequestration density could help carbon fixation process. On the contrary, species with negative carbon sequestration density could aggravate threat posed by GHGs emission.

3.5 GHGs emission

The resources GHGs emission of four designed scenarios were illustrated in **Figure 7**. The Scenario 1 illustrated the GHGs emission of current Tsui Ping River where no vegetation was planted (Deign I in **Figure 1**); Scenarios 2 and 3 represented the watershed restoration approaches with increased planting areas (Deign II and III, respectively) and best performed plant; and Scenarios 4 showed the worse performing plant species with largest planting area (Deign III). As a result, the total GHGs emission of Scenarios 1 through 4 were 0.15066, 0.11655, 0.08238 and 0.17551 kg CO_2-e/m^3, respectively. The CH_4 emission from decayed biomass and COD contributed the principal GHGs emission was 0.19844 kg CO_2-e/m^3 in all scenarios. Reduced CH_4 by DO accounted for major proportion of reducing GHGs emission, which is -0.05013 kg CO_2-e/m^3.

Compared scenario 1 with 2, 3 and 4, vegetation growth played a significant role in terms of effecting GHGs emission. For Scenario 2, GHGs reduction by C and N sequestration from CT growth were -0.00183 and -0.02998 kg CO_2-e/m^3, respectively. GHGs from C and N sequestration in scenario had more significant impact on GHGs reduction, which were -0.00366 and -0.06002 kg CO_2-e/m^3, respectively, where there was more available area for scenario 3. However, C and N sequestration from EH growth in scenario 4 strengthened the GHGs emission, which were 0.0015 and 0.02424 kg CO_2-e/m^3, respectively. Some important parameters contributing to GHGs emission from improper control of wastewater discharges in other studies (Zhuang et al., 2020b), *i.e.*, GHGs from eutrophication, N_2O from stormwater, reduced N_2O from stormwater by vegetation and Reduced GHGs from eutrophication by vegetation, were calculated, but were less significant in this study (data not presented here). Compared to scenario 1 without vegetation, GHGs emission of scenario 4 more than current design. This result suggesting that cultivating vegetation would aggravate GHGs emission if wrong plant species were adopted.

4. Conclusion

This study demonstrated that the degradations of organic carbon, unlike ammonia nitrogen, seems not to be a critical factor supporting plant growths. The relation between half-life of NH_4^+ and increased biomass showed similar slope in shoot and leaves Slope in shoot (-0.301) and leaves (-0.279) in batch experiments presented sharper trend than that in continuous experiments (shoot in -0.232 and leaves in -0.230). The results of half-life coefficients ($t_{1/2}$) of pollutants treated demonstrated that five particular plant species (*i.e.*, CT, TD, CrA, PA, KO and AC_c) have more significant capabilities for water purification. The gradual decreases of COD half-life in freshwater (1.04-2.26 days), brackish water (2.33-8.80 days), and sea water (27.19-75.08 days) plants indicated that increased salinity or plant species with high tolerances to sea water showed less tendency absorbing the COD. CT, CrA and PA were identified being crucial contributors to carbon accumulation in watershed through both the direct and indirect manners, resulting in approximately 313.90, 236.07 and 141.19 g/m^2 of carbon sequestration during 30-day cultivation, respectively. However, EH and SS were regarded to be improper species for alleviating GHGs emission in watershed, with expected -128.2 and 38.24 g/m^2 carbon storage in 30-day continuous flow processes. The two plants suffered from frequent defoliation or stand fall if it cannot resist external environmental turbulences. Turning embankment and water surface into plantation ground with more planting area can further enhance water purification capacities and reduce GHGs emission. However, it should be emphasized again that pollutant removal shall serve only as an extra function of greening and cannot be treated as the main water purification approach for watershed restoration.

Acknowledgments

This study was supported by the Hong Kong Research Grant Council, General Research Fund (GRF 15212319); Innovation and Technology Commission (GHP/042/18GD); and the Research Institute for Sustainable Urban Development (RISUD, PolyU 1-BBW6) of the Hong Kong Polytechnic University.

Figures Caption

Figure 1 Conceptual diagram of the proposed study

Figure 2 Experimental set-ups for (a) batch experiment; (b) continuous flow experiment

Figure 3 Physical properties of plant species cultivated in Zone A, B and C over 30-day experiments

Figure 4 Pollutants per unit biomass in batch experiments in Zone A, B and C (a, b, and c for Zone A; d, e, and f for Zone B; g, h, and I for Zone C)

Figure 5 Half-life ($t_{1/2}$) of pollutants treated by 21 plant species

Figure 6 Correlations between half-life of pollutants and increased biomass

Figure 7 GHGs distributions in 4 planting scenarios

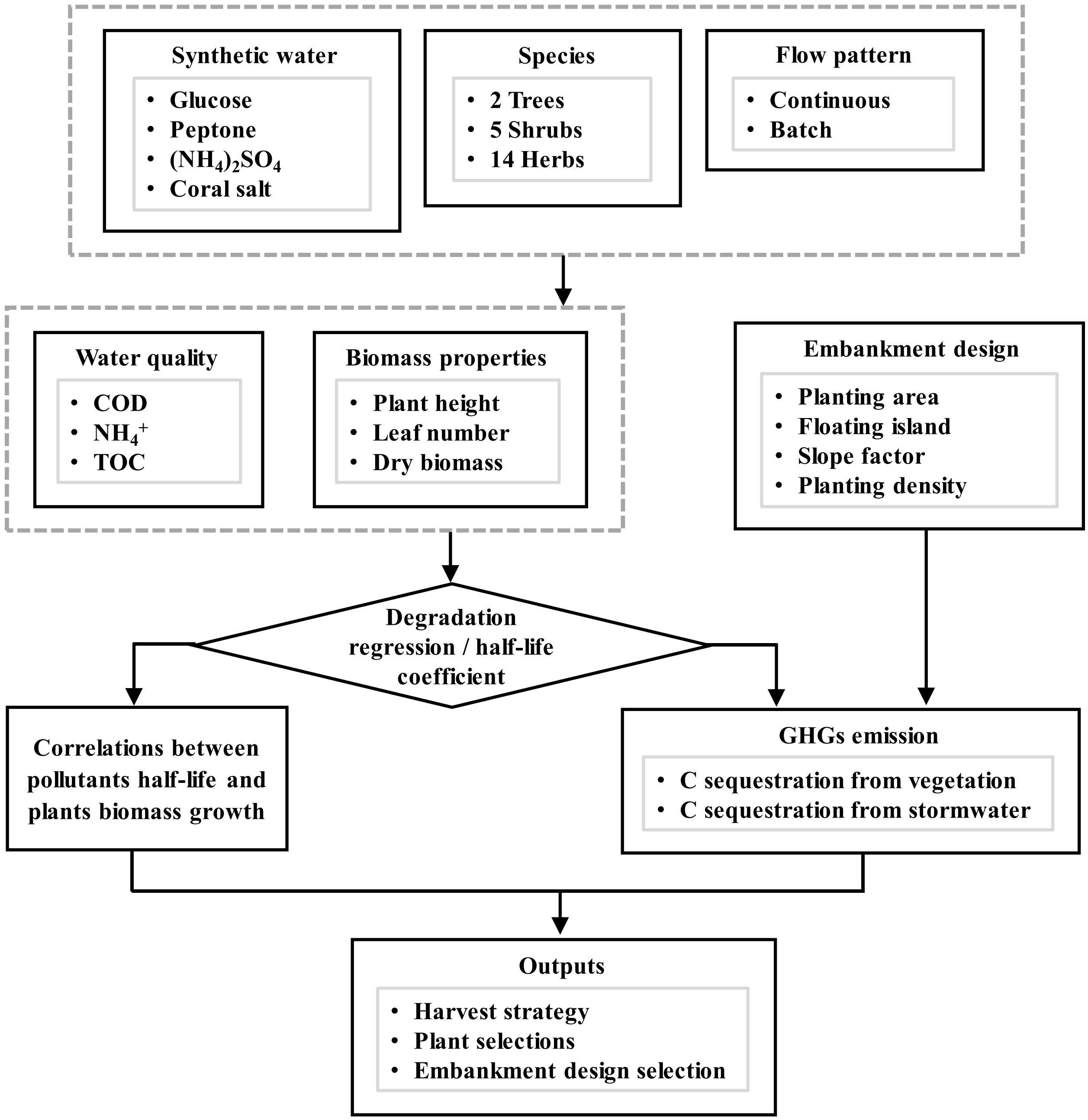

Figure 1 Conceptual diagram of the proposed study

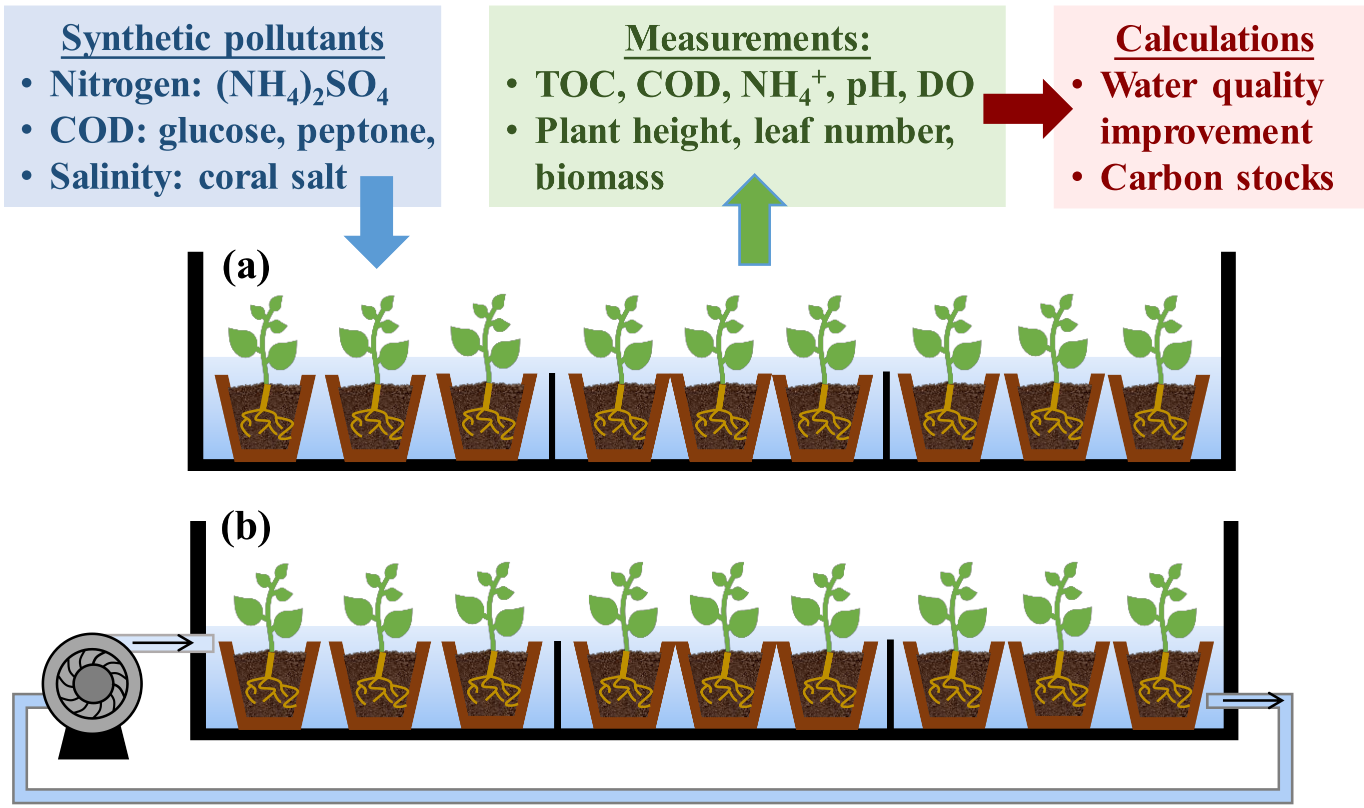

Figure 2 Experimental set-ups for (a) batch experiment; (b) continuous flow experiment

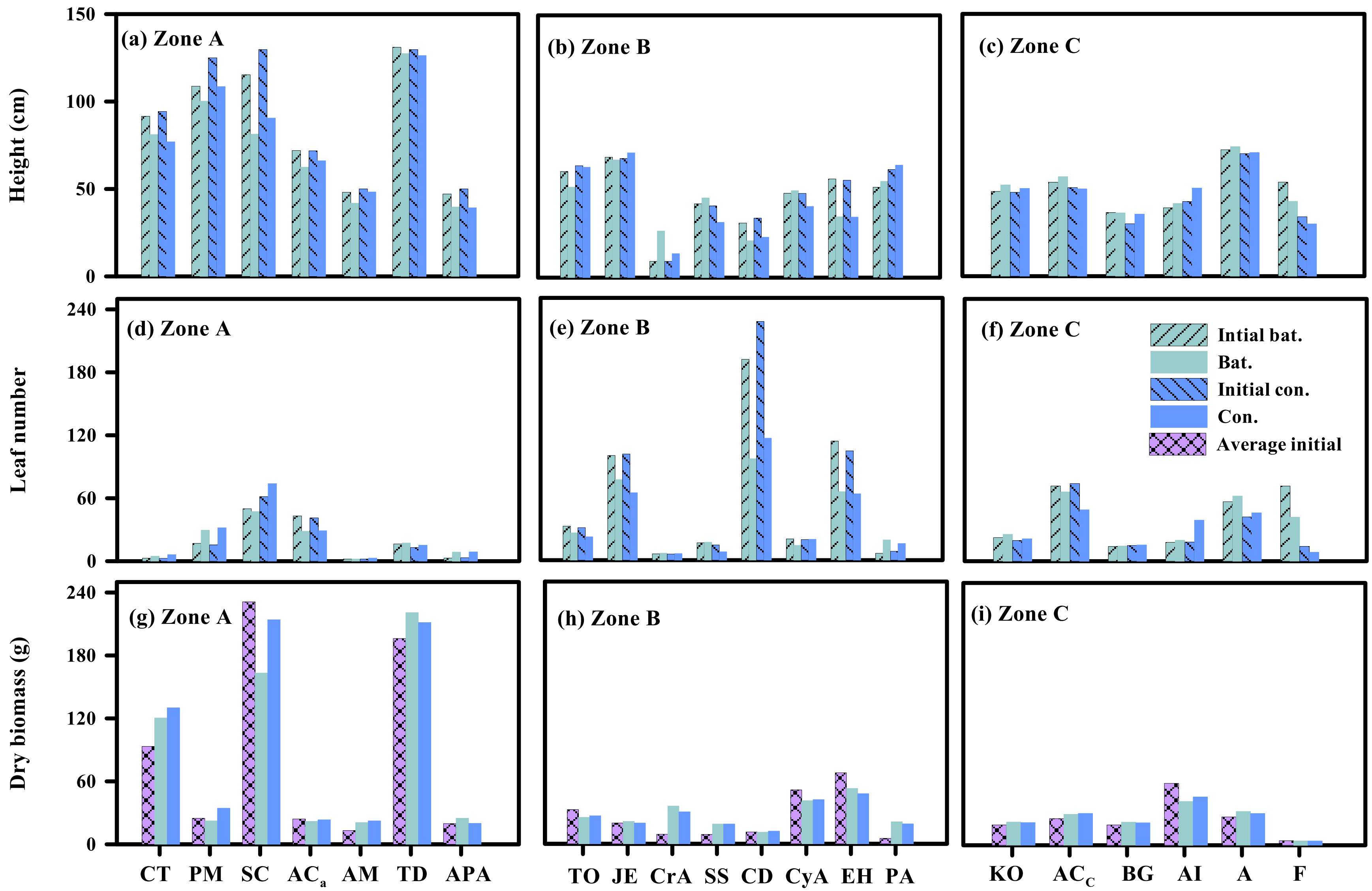

Figure 3 Physical properties of plant species cultivated in Zone A, B and C over 30-day experiments

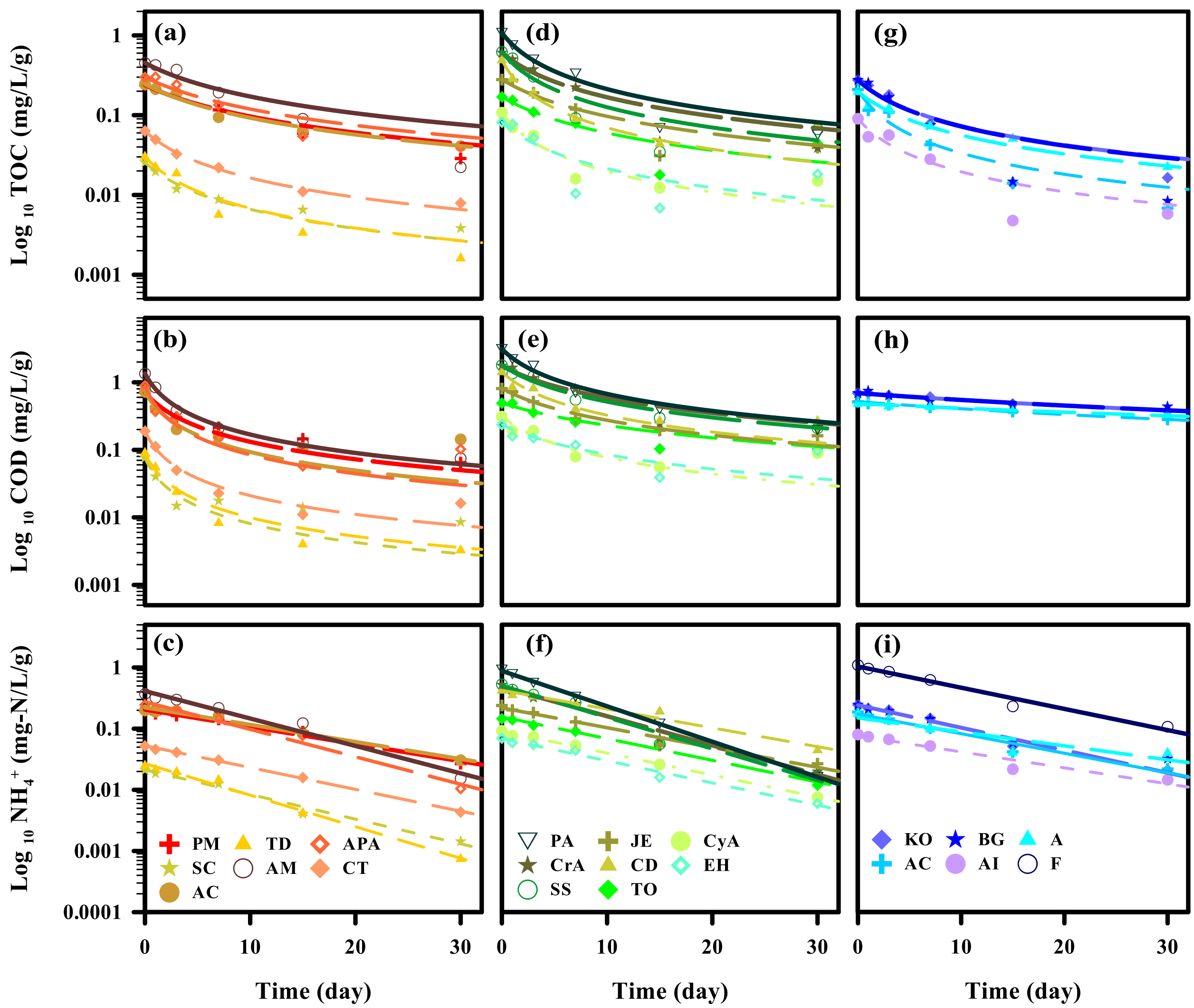

Figure 4 Pollutants per unit biomass in batch experiments in Zone A, B and C (a, b, and c for Zone A; d, e, and f for Zone B; g, h, and I for Zone C)

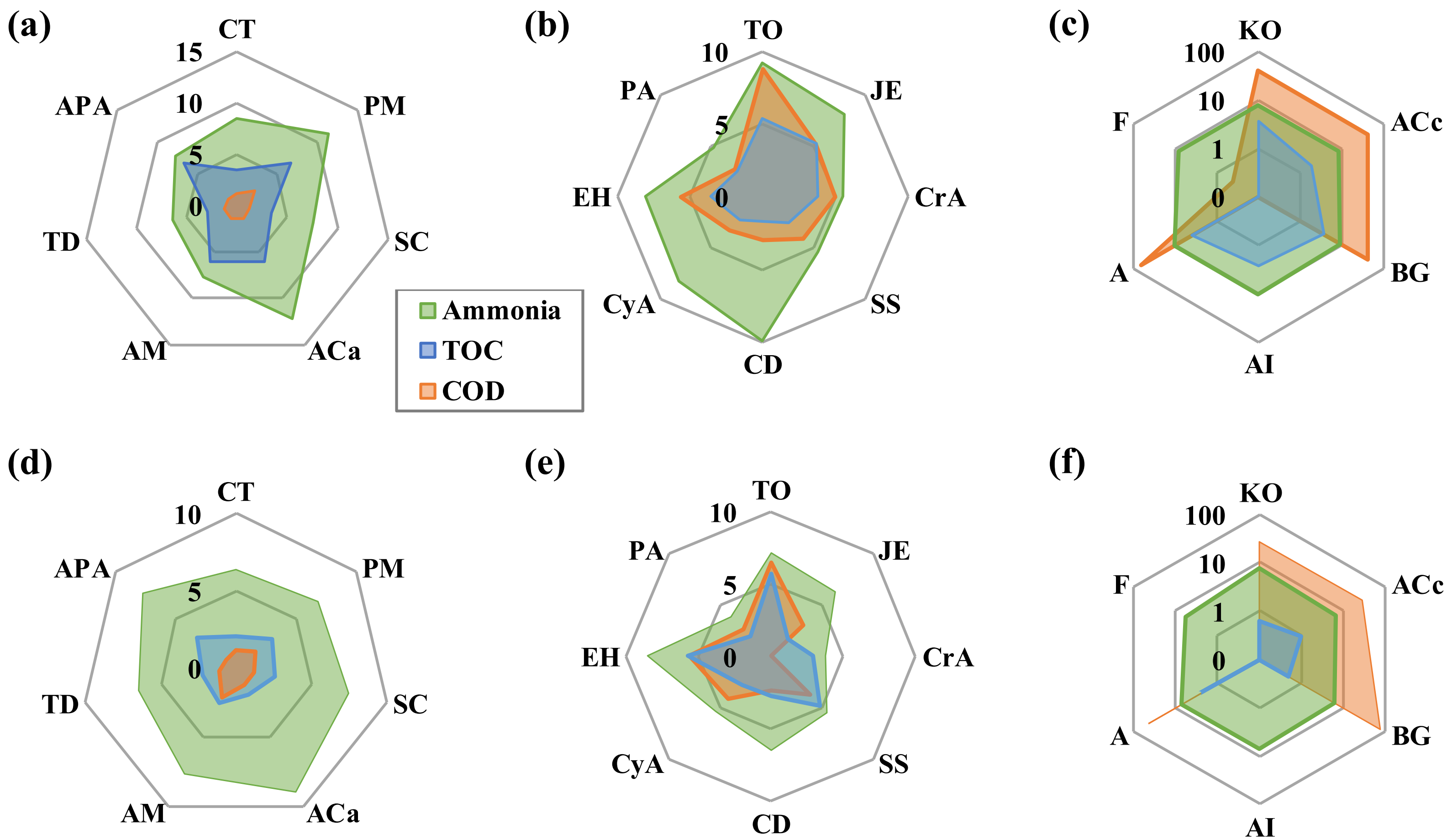

Figure 5 Half-life ($t_{1/2}$) of pollutants treated by 21 plant species

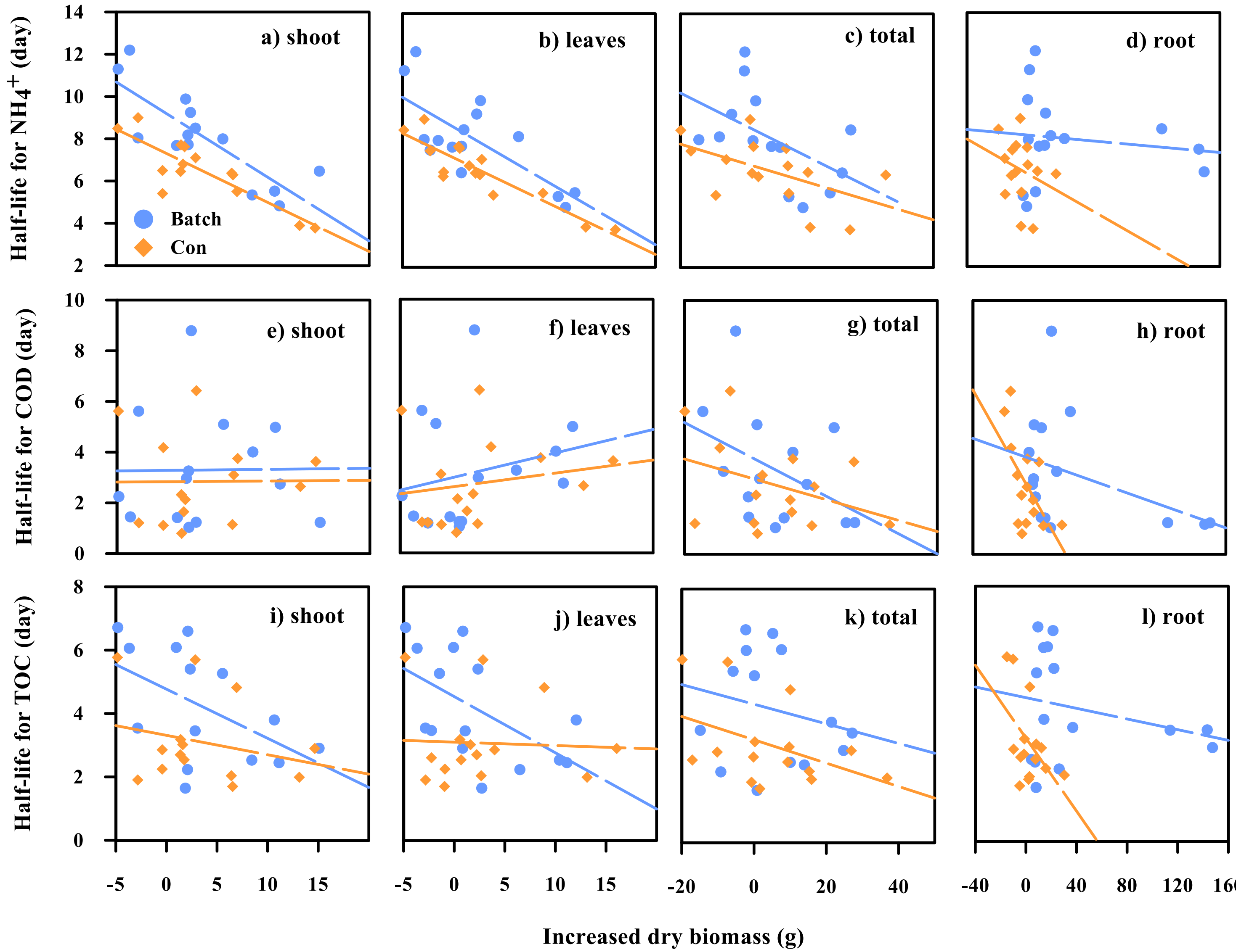

Figure 6 Correlations between half-life of pollutants and increased biomass

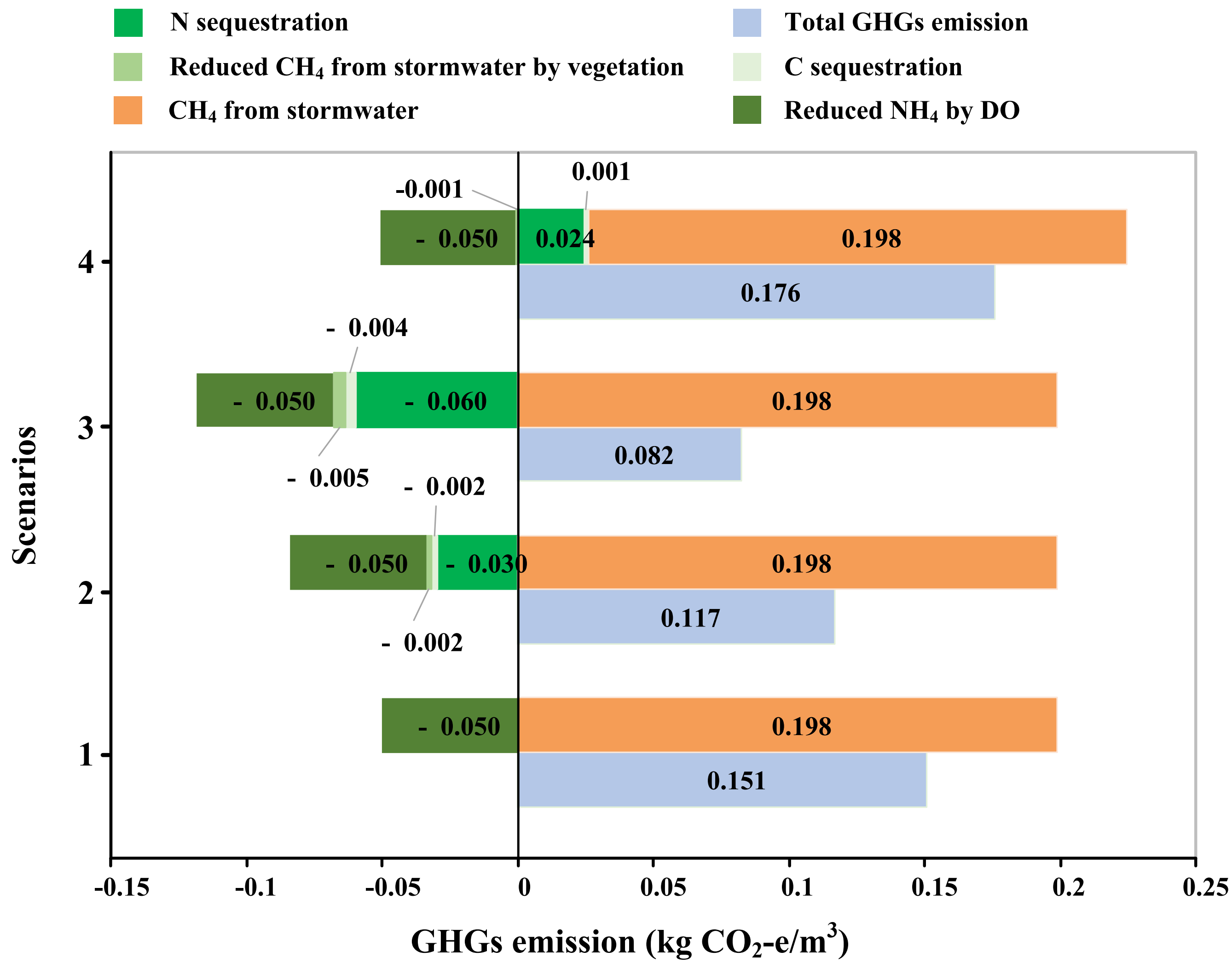

Figure 7 GHGs distributions in 4 planting scenarios

Table 1. Properties of Zone A, B and C

Items		Zone A	Zone B	Zone C
NH_4^+ (mg/L)		16.4	16.4	16.4
Glucose (mg/L)		44	44	44
Peptone (mg/L)		164	164	164
Salinity (ppt)		0	5	15
Flowrate (L/S)	Batch	0	0	0
	Continuous	3~8	3~8	3~8
Plant species		*Colocasia tonoimo* (CT)	*Typha orientalis* (TO)	*Kandelia obovate* (KO)
		Panicum maximum (PM)	*Juncus effuses* (JE)	*Aegiceras corniculatum* (AC_c)
		Saururus chinensis (SC)	*Crinum asiaticum* (CrA)	*Bruguiera gymnorrhiza* (BG)
		Acorus calamus (AC_a)	*Scaevola sericea* (SS)	*Acanthus ilicifolius* (AI)
		Alocasia macrorrhizos (AM)	*Commelina diffusa* (CD)	*Clerodendrum inerme* (A)
		Thalia dealbata (TD)	*Cyperus alternifolius* (CyA)	*Acrostichum aureum* (F)
		Alisma plantago-aquatica (APA)	*Equisetum hyemale* (EH)	
			Phragmites australis (PA)	

Table 2. Carbon and nitrogen sequestration parameters

Location	Species	Type	Dry biomass per stand over 30 days in bat. (g)			Dry biomass per stand at day 30 in con. (g)			Carbon content (%)			Density ρ (m^2/stand)	C sequestration density in 30 days (g/m^2)		N sequestration density in 30 days (g/m^2)	
			Root	Stem	Leaves	Root	Stem	Leaves	Root fr	Stem fs	Leaves fl		Bat.	Con.	Bat.	Con.
Zone A	CT	herb	114.00	4.25	2.25	120.08	6.25	3.83	42.45	42.41	44.73	20.00	231.12	313.90	16.69	22.64
	PM	herb	9.48	/	12.97	15.11	/	19.39	42.45	42.41	44.73	20.00	-21.63	83.53	-1.40	5.97
	SC	herb	143.33	17.72	/	192.67	19.17	2.25	42.45	42.41	44.73	15.00	-432.84	-109.48	-31.35	-7.86
	AC[a]	herb	14.00	/	8.00	14.63	/	8.83	42.45	42.41	44.73	20.00	-20.07	-7.31	-1.32	-0.43
	AM	herb	17.03	2.63	1.07	17.94	2.67	1.82	42.45	42.41	44.73	20.00	64.57	79.41	4.66	5.71
	TD	herb	147.50	55.75	17.67	153.54	42.00	15.92	42.45	42.41	44.73	15.00	157.80	97.05	11.40	7.03
	APA	herb	21.42	2.07	1.48	17.17	1.66	1.19	42.45	42.41	44.73	20.00	44.51	2.29	3.18	0.15
Zone B	TO	herb	22.14	/	4.65	20.14	/	5.15	42.45	42.41	44.73	20.00	-48.11	-60.62	-3.54	-4.46
	JE	herb	8.44	7.00	4.46	8.94	7.50	4.96	42.45	42.41	44.73	20.00	0.16	13.12	0.06	0.98
	CrA	herb	14.22	1.39	14.95	15.72	1.39	18.95	42.45	42.41	44.73	20.00	187.55	236.07	13.16	16.55
	SS	shrub	4.39	1.96	12.60	5.89	1.96	11.10	47.43	31.36	19.00	15.00	31.84	38.24	1.27	1.22
	CD	herb	8.02	0.86	3.28	7.52	0.86	2.78	42.45	42.41	44.73	20.00	8.49	-0.22	0.52	-0.09
	CyA	herb	26.27	4.40	11.51	27.77	4.40	9.01	42.45	42.41	44.73	20.00	-74.97	-84.60	-5.62	-6.24
	EH	herb	37.03	/	15.85	34.03	/	13.85	42.45	42.41	44.73	15.00	-95.68	-128.20	-6.84	-9.15
	PA	herb	7.21	/	11.87	7.21	/	13.87	42.45	42.41	44.73	20.00	123.30	141.19	8.54	9.77
Zone C	KO	tree	6.88	12.62	2.68	6.70	12.29	2.61	47.43	32.42	20.91	15.00	15.24	12.10	0.26	0.21
	AC[c]	shrub	7.78	11.67	10.11	8.00	12.00	10.40	47.43	31.36	19.00	20.00	26.49	31.77	0.69	0.83
	BG	tree	4.49	14.87	4.49	4.39	14.52	4.39	47.43	32.42	20.91	20.00	5.67	1.95	0.11	0.04
	AI	shrub	9.68	24.32	7.79	10.66	26.78	8.58	47.43	31.36	19.00	15.00	-84.58	-63.85	-2.13	-1.61
	A	shrub	8.00	16.70	7.57	7.51	15.68	7.11	47.43	31.36	19.00	20.00	34.14	21.45	0.86	0.54
	F	shrub	0.96	/	3.21	0.95	/	3.18	47.43	31.36	19.00	20.00	-0.83	-1.03	-0.03	-0.03

Table 3. Properties of four planting scenarios

Scenarios	Embankment design	Planting area (m^2)	Species	Density (stand/m^2)
1	A	0	/	/
2	B	2743	CT	20
3	C	4575	CT	24
4	C	4575	EH	18

References

Baleta, J., Mikulčić, H., Klemeš, J.J., Urbaniec, K. and Duić, N. 2019. Integration of energy, water and environmental systems for a sustainable development. Journal of Cleaner Production 215, 1424-1436.

Breen, P.F. 1990. A mass balance method for assessing the potential of artificial wetlands for wastewater treatment. Water Research 24(6), 689-697.

Chan, K.-L., Dong, C., Wong, M.S., Kim, L.-H. and Leu, S.-Y. 2018. Plant chemistry associated dynamic modelling to enhance urban vegetation carbon sequestration potential via bioenergy harvesting. Journal of Cleaner Production 197, 1084-1094.

Chandrasena, G., Shirdashtzadeh, M., Li, Y., Deletic, A., Hathaway, J. and McCarthy, D. 2017. Retention and survival of E. coli in stormwater biofilters: role of vegetation, rhizosphere microorganisms and antimicrobial filter media. Ecological Engineering 102, 166-177.

Chen, W.Y. and Cho, F.H.T. 2019. Environmental information disclosure and societal preferences for urban river restoration: Latent class modelling of a discrete-choice experiment. Journal of Cleaner Production 231, 1294-1306.

Davis, A.P., Hunt, W.F., Traver, R.G. and Clar, M. 2009. Bioretention technology: Overview of current practice and future needs. Journal of Environmental Engineering 135(3), 109-117.

Ge, Z., Feng, C., Wang, X., Zhang, J. and Biodegradation 2016. Seasonal applicability of three vegetation constructed floating treatment wetlands for nutrient removal and harvesting strategy in urban stormwater retention ponds. International Biodeterioration 112, 80-87.

Hu, M., Zhang, X., Li, Y., Yang, H. and Tanaka, K. 2019. Flood mitigation performance of low impact development technologies under different storms for retrofitting an urbanized area. Journal of Cleaner Production 222, 373-380.

Kauffman, J.B., Beschta, R.L., Otting, N. and Lytjen, D. 1997. An ecological perspective of riparian and stream restoration in the western United States. Fisheries 22(5), 12-24.

Keizer-Vlek, H.E., Verdonschot, P.F., Verdonschot, R.C. and Dekkers, D. 2014. The contribution of plant uptake to nutrient removal by floating treatment wetlands. Ecological Engineering 73, 684-690.

Ladislas, S., Gerente, C., Chazarenc, F., Brisson, J. and Andres, Y. 2013. Performances of two macrophytes species in floating treatment wetlands for cadmium, nickel, and zinc removal from urban stormwater runoff. Water, Air, Soil Pollution 224(2), 1408.

Li, Y.C., Zhang, D.Q. and Wang, M. 2017. Performance Evaluation of a Full‐Scale Constructed Wetland for Treating Stormwater Runoff. CLEAN–Soil, Air, Water 45(11), 1600740.

Lin, S.-S., Shen, S.-L., Zhou, A. and Lyu, H.-M. 2020. Sustainable development and environmental restoration in Lake Erhai, China. Journal of Cleaner Production, 120758.

Loperfido, J.V., Noe, G.B., Jarnagin, S.T. and Hogan, D.M. 2014. Effects of distributed and centralized stormwater best management practices and land cover on urban stream hydrology at the catchment scale. Journal of Hydrology 519, 2584-2595.

Lopez-Ponnada, E.V., Lynn, T.J., Ergas, S.J. and Mihelcic, J.R. 2020. Long-term field performance of a conventional and modified bioretention system for removing dissolved nitrogen species in stormwater runoff. Water Research 170, 115336.

Ma, S., He, F., Tian, D., Zou, D., Yan, Z., Yang, Y., Zhou, T., Huang, K., Shen, H. and Fang, J. 2018. Variations and determinants of carbon content in plants: a global synthesis. Biogeosciences 15(3), 693.

Nordman, E.E., Isely, E., Isely, P. and Denning, R. 2018. Benefit-cost analysis of stormwater green infrastructure practices for Grand Rapids, Michigan, USA. Journal of Cleaner Production 200, 501-510.

Pavolová, H., Bakalár, T., Kudelas, D. and Puškárová, P. 2019. Environmental and economic assessment of rainwater application in households. Journal of Cleaner Production 209, 1119-1125.

Perrin, A., Basset-Mens, C., Huat, J. and Gabrielle, B. 2017. The variability of field emissions is critical to assessing the environmental impacts of vegetables: A Benin case-study. Journal of Cleaner Production 153, 104-113.

Ralston, B.E. and Sarr, D.A. (2017) Case Studies of Riparian and Watershed Restoration in the Southwestern United States: Principles, Challenges, and Successes, US Department of the Interior, US Geological Survey.

Reich, P.B., Tjoelker, M.G., Machado, J.-L. and Oleksyn, J. 2006. Universal scaling of respiratory metabolism, size and nitrogen in plants. Nature 439(7075), 457-461.

Revitt, D., Shutes, R., Llewellyn, N. and Worrall, P. 1997. Experimental reedbed systems for the treatment of airport runoff. Water Science Technology 36(8-9), 385-390.

Rogers, K., Breen, P. and Chick, A. 1991. Nitrogen removal in experimental wetland treatment systems: evidence for the role of aquatic plants. Research Journal of the Water Pollution Control Federation, 934-941.

Roni, P., Beechie, T.J., Bilby, R.E., Leonetti, F.E., Pollock, M.M. and Pess, G.R. 2002. A review of stream restoration techniques and a hierarchical strategy for prioritizing restoration in Pacific Northwest watersheds. North American Journal of Fisheries Management 22(1), 1-20.

Rosso, D. and Stenstrom, M.K. 2008. The carbon-sequestration potential of municipal wastewater treatment. Chemosphere 70(8), 1468-1475.

Rozema, J., van de Staaij, J., Björn, L.O. and Caldwell, M. 1997. UV-B as an environmental factor in plant life: stress and regulation. Trends in Ecology & Evolution 12(1), 22-28.

Sharrock, S. and Jackson, P.W. 2017. Plant Conservation and the Sustainable Development Goals: A Policy Paper Prepared for the Global Partnership for Plant Conservation1. Annals of the Missouri Botanical Garden 102(2), 290-302.

Sun, G., Zhao, Y. and Allen, S. 2005. Enhanced removal of organic matter and ammoniacal-nitrogen in a column experiment of tidal flow constructed wetland system. Journal of Biotechnology 115(2), 189-197.

Viana, H., Vega-Nieva, D., Torres, L.O., Lousada, J. and Aranha, J. 2012. Fuel characterization and biomass combustion properties of selected native woody shrub species from central Portugal and NW Spain. Fuel 102, 737-745.

Vymazal, J. (1995) Algae and element cycling in wetlands, Lewis Publishers Inc.

Wu, S., Zhang, D., Austin, D., Dong, R. and Pang, C. 2011. Evaluation of a lab-scale tidal flow constructed wetland performance: oxygen transfer capacity, organic matter and ammonium removal. Ecological Engineering 37(11), 1789-1795.

Xu, B., Wang, X., Liu, J., Wu, J., Zhao, Y. and Cao, W. 2017. Improving urban stormwater runoff quality by nutrient removal through floating treatment wetlands and vegetation harvest. Scientific Reports 7(1), 1-11.

Xu, C., Jia, M., Xu, M., Long, Y. and Jia, H. 2019. Progress on environmental and economic evaluation of low-impact development type of best management practices through a life cycle perspective. Journal of Cleaner Production 213, 1103-1114.

Yang, Z., Zheng, S., Chen, J. and Sun, M. 2008. Purification of nitrate-rich agricultural runoff by a hydroponic system. Bioresource Technology 99(17), 8049-8053.

Zheng, B., Huang, G., Liu, L., Zhai, M. and Guan, Y. 2019. Metabolism of urban wastewater: ecological network analysis for Guangdong Province, China. Journal of Cleaner Production 217, 510-519.

Zhuang, H., Guan, J., Leu, S.-Y., Wang, Y. and Wang, H. 2020a. Carbon Footprint Analysis of Chemical Enhanced Primary Treatment and Sludge Incineration for Sewage Treatment in Hong Kong. Journal of Cleaner Production, 122630.

Zhuang, H., Guan, J., Leu, S.-Y., Wang, Y. and Wang, H. 2020b. Carbon footprint analysis of chemical enhanced primary treatment and sludge incineration for sewage treatment in Hong Kong. Journal of Cleaner Production 272, 122630.

Strategic Planting for Watershed Restoration in Coastal Urban Environment – Toward Carbon Sequestration by Stormwater Improvement

Xiaojing Tang[a], Ka-Lai Chan[a], Shazia Farzana[a], Onyx W.H. Wai[a,b], and Shao-Yuan Leu[a,b,c*]

[a] Department of Civil and Environmental Engineering, The Hong Kong Polytechnic University, Hung Hom, Kowloon, Hong Kong SAR;

[b] Research Institute for Sustainable Urban Development (RISUD), The Hong Kong Polytechnic University;

[c] Research Institute for Smart Energy (RISE), The Hong Kong Polytechnic University;

[*] Correspondence: Department of Civil and Environmental Engineering, the Hong Kong Polytechnic University, Hung Hom, Kowloon, Hong Kong SAR; Phone: 852-3400-8322; Fax: 852-2334-6389; E-mail: syleu@polyu.edu.hk (S,-Y. Leu)

Credit Author Statement

Tang and Farzana – designed, carried out the experiments and drafted the manuscript; Chan – constructed the model and performed the simulations; Wai and Leu – supervised the research and edited the manuscript.

Declaration of interests

☒ The authors declare that they have no known competing financial interests or personal relationships that could have appeared to influence the work reported in this paper.

☐The authors declare the following financial interests/personal relationships which may be considered as potential competing interests:

Declarations of interest: none